PROCEEDINGS OF SCIENCE

Performance of the LHCb Tracking Detectors

Mark TOBIN[*†]
Universitaet Zuerich (CH)
E-mail: Mark.Tobin@cern.ch

The LHCb experiment is making high-precision measurements of CP violation and searching for New Physics using the enormous flux of beauty and charmed hadrons produced at the LHC. The detector includes a high precision tracking system consisting of a silicon-strip vertex detector surrounding the pp interaction region, a large-area silicon-strip detector located upstream of a dipole magnet, and three stations of silicon-strip detectors and straw drift tubes placed downstream. The performance of the individual silicon-strip detectors will be discussed together with the overall performance of the full tracking system.

The 21st International Workshop on Vertex Detectors
16-21 September 2012
Jeju, Korea

[*]Speaker.
[†]On behalf of the LHCb collaboration.

PoS(Vertex 2012)047

1. Introduction

The LHCb experiment [1] is a single arm spectrometer designed to study heavy flavour physics in decays of B-mesons. The primary goal of LHCb is to search for indirect evidence of new physics in CP violation and rare decays of b and c hadrons. At the LHC, b-pairs are predominantly produced close to the beam direction. The LHCb detector covers a pseudorapidity range of 2 to 5. The fraction of b-pairs produced in the LHCb acceptance at $\sqrt{s} = 7$ TeV is around 27% [2]. One important design requirement of the detector is the ability to measure the position of primary and secondary vertices with a high precision in order to separate b-hadron decays from background. This is done by the LHCb tracking system which also provides a high resolution measurement of the particle momentum.

2. LHCb Tracking System

The LHCb tracking system consists of the Vertex Locator (VELO), a silicon micro-strip detector surrounding the proton-proton interaction region; the Tracker Turicensis (TT), a large area silicon micro-strip detector located upstream of the magnet; the Inner Tracker (IT), a silicon micro-strip detector which covers the region around the beam with the highest flux downstream of the magnet; the Outer Tracker (OT), a straw-tube detector covering the acceptance outside the IT; and a dipole magnet with a bending power of around 4 Tm. The TT and IT form the Silicon Tracker (ST). The rest of this paper will focus on the performance of the VELO and the ST.

The VELO consists of 42 modules arranged perpendicular to the beam around the interaction region. It is divided into two halves which are contained in a secondary vacuum and separated from the primary vacuum by a 300 μm aluminium foil. This so-called RF foil also shields the detector from possible radio frequency (RF) pick-up from the beam. The two halves can be retracted to positions 30 mm from the interaction region during the beam injection. The shape of the foil allows the halves to overlap when the detector is in its closed position centred around the interaction region with the closest point of the RF foil 5 mm away from the beam axis.

A VELO module consists of two 300 μm thick semi-circular n^+-on-n oxygenated silicon sensors with 2048 strips. One sensor measures the radial coordinate, R, and the other measures the azimuthal angle, Φ. The R-sensor is segmented in 45° quadrants and has a pitch that increases linearly from 40 μm at the inner radius (8.13 mm) to 101.6 μm at the outer radius (42mm). The Φ sensor has radial strips with a small stereo angle split into 683 short inner strips and 1365 long outer strips. The pitch of the Φ sensors varies from 35 to 101 μm and the strips in each region are skewed in opposite directions by 10° and 20°. The R-Φ geometry was chosen to allow fast reconstruction of tracks and vertices in the LHCb trigger. The sensors are mounted on a double sided hybrid consisting of a substrate with a Thermal Pyrolytic Graphite (TPG) core cloaked in carbon fibre onto which a kapton circuit is laminated on each side. The strips are routed via a double metal layer on the sensor to the hybrid where there are 16 Beetle front-end chips [4].

The Silicon Tracker is a silicon micro-strip detector with a sensitive area of approximately 12 m^2 and a total of 272k readout channels. It consists of two detectors: the Tracker Turicensis (TT), a 150 cm wide and 130 cm high tracking station covering the full LHCb acceptance upstream

of the LHCb magnet; and the Inner Tracker (IT), which covers a 120 cm by 40 cm cross-shaped region in the centre of three planar tracking stations downstream of the magnet.

The Tracker Turicensis has four detection layers orientated at (0°, +5°, -5°, 0°) with respect to the vertical axis. The detector is constructed from 500 μm thick p-on-n sensors with a pitch of 183 μm. Sensors are bonded together to make readout sectors with 1, 2, 3 or 4 sensors resulting in long readout strips (up to 37 cm). The single sensor sectors are closest to the beam-pipe in the region of highest particle flux while the other sectors are arranged such that the maximum occupancy in each sector is around 1%. There are 280 readout sectors in the TT and a total of 143360 readout channels.

The three Inner Tracker stations each consist of four independent boxes arranged around the beam pipe. Each box contains four detection layers with the same orientation as those in the TT. Detector modules in the boxes either side of the beam pipe use 410 μm thick p-on-n sensors and have a length of 22 cm while those in the boxes above and below the beam pipe are 11 cm long and 320 μm thick. The strip pitch is 198 μm for both sensor thicknesses. There are 336 readout sectors in IT and a total of 129024 readout channels. The IT reconstructs 20% of all tracks passing through LHCb despite covering only 1.2% of the total acceptance.

The reconstruction of tracks is performed in stages. First, tracks are reconstructed as straight lines using the R sensors of the VELO. Then, hits from the Φ sensors are added to these tracks. Two different algorithms are used to combine these VELO tracks with hits in the other tracking stations. The first method propagates the VELO tracks through the magnetic field and adds hits in the downstream tracking stations. The second method makes track seeds in the tracking stations and then tries to propagate these tracks in the opposite direction and match them to the VELO tracks. Finally, hits from the TT station are added to the track to improve the momentum resolution and reject incorrect combinations of hits. Tracks which traverse all of the tracking stations are called *Long* tracks and these tracks form the core of the reconstruction for most physics events. Tracks with no measurements in the VELO, for example those from K^0_S decays, are called *Downstream* tracks and those with no hits in any tracking station after the TT are called *Upstream* tracks. The fitting of the tracks is based on a bi-directional Kalman filter which takes into account multiple scattering of particles and energy loss in the detector material.

3. LHCb Operation and Performance

The LHCb detector was designed to collect data from proton-proton collisions at the LHC with a centre-of-mass energy of 14 TeV and an instantaneous luminosity ($\mathscr{L}$) around $2 \times 10^{32}/\text{cm}^2/\text{s}$. In this scheme, there would be 2808 bunches separated by 25 ns with the average number of visible proton-proton interactions per bunch crossing (μ) equal to 0.4. The nominal LHC filling scheme has not yet been achieved and the current bunch spacing is 50 ns. The centre-of-mass energy was 7 TeV and 8 TeV during 2011 and 2012 respectively. The nominal luminosity, however, could be reached, and indeed exceeded, by allowing pile-up events which contain more than a single pp interaction. The luminosity at LHCb can be controlled by changing the beam separation until the required rate is achieved. The rate can be maintained by further reducing the beam separation during a fill in a process known as "luminosity levelling". The data taken in 2011 were collected with different target luminosities and pile-up. The majority of the data collected in 2012

has $\langle \mathscr{L} \rangle \approx 4 \times 10^{32}/\mathrm{cm}^2/\mathrm{s}$ and $\langle \mu \rangle \approx 1.7$. The average value of $\mathscr{L}$ and μ during each fill are shown in figure 1.

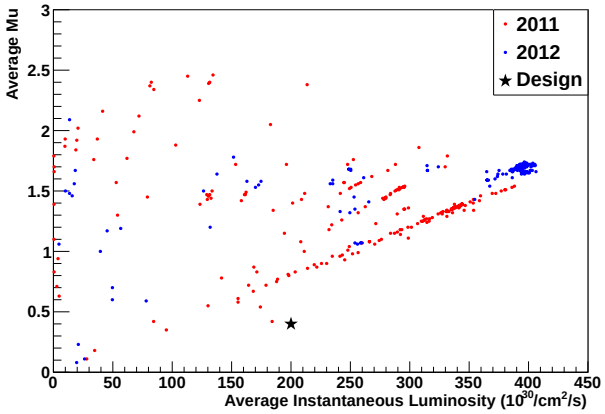

Figure 1: Average number of visible pp interactions (mu) versus average instantaneous luminosity for the different fills in 2011 (red) and 2012 (blue). The design value is indicated by a star.

The nominal running conditions in 2011 and 2012 are very different from the design conditions. However, it was shown offline that it was possible to take data with several pile-up interactions without any degradation in the performance of the detector. The choice of the running conditions is influenced by limitations in the readout speed, the trigger configuration, and occupancies in the different sub-detectors. The output rate of the software trigger running in 2012 is around 4 kHz which is double the design value! The total integrated luminosity recorded during 2011 was 1.11 fb^{-1}, whilst 1.34 fb^{-1} had been collected in 2012 at the time of the conference.

4. VELO Performance

The analogue data from one sensor is digitised by four analogue receiver cards and then pre-processed by four FPGAs on a TELL1 readout board [5]. The data processing involves pedestal subtraction, channel re-ordering, common mode noise suppression and clustering. The fraction of working channels was 99.27% at the time of this conference.

The noise on the chip depends on the input capacitance which is proportional to the length of the strip. The noise increases in the R sensors as a function of the radius. The noise is shown in figure 2 as a function of the strip number for the R sensor. The strip number increases as a function of the radius for each of the four segments in the sensor. The Φ sensor has three distinct types of strips; the short inner strips; the long outer strips, which are alternately overlaid with a routing line which increase the capacitance of the strip. This leads to the three distinct bands of noise that can be seen in figure 2.

The typical signal is measured by looking at the charge distribution of clusters on tracks and fitting a Landau convolved with a Gaussian to the peak region. The distribution of the signal value is shown in figure 3. The most probable value of the Landau fit is used to calculate the signal to noise ratio. This is also shown in figure 3 and is seen to vary as a function of the radius.

The spatial alignment of the VELO was made using two different methods: a non-iterative method using matrix inversion based on Millepede [8]; and a global χ^2 minimisation based on

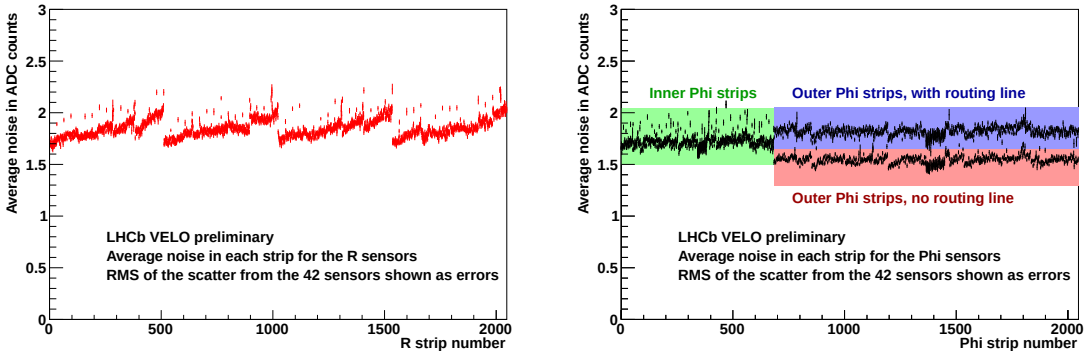

Figure 2: Noise per strip as a function of the strip number for R sensors (left) and Φ sensors (right).

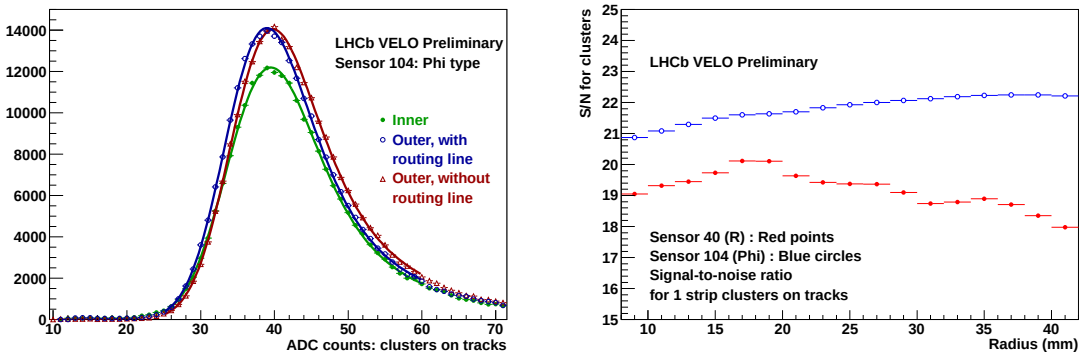

Figure 3: Cluster charge in ADC counts for a Φ sensor (left) and signal to noise ratio as a function of radius (right).

Kalman track residuals [9]. The initial alignment was based on high precision survey measurements and a first track alignment was made using particles induced during LHC injection tests [10]. Further improvements were made using data taken during proton-proton collisions. The results from the two different methods are in agreement.

The alignment is constantly monitored as the VELO halves are retracted during the beam injection and then centred around the beam for each fill. This fully automated procedure takes around 210 seconds from the declaration of stable beams and has been performed over 500 times. The stability of the alignment of one half with respect to the other is measured by reconstructing the primary vertex using each half separately. The distance between the primary vertices reconstructed by each half is shown in figure 4 as a function of the run number. During 2010, the relative half alignment was stable within 5 μm along the main direction of the VELO closing, the x-direction.

The spatial resolution depends on the strip pitch and charge sharing between the strips. The charge sharing depends on the projected angle of the track and the operation voltage. The projected angle is defined as the angle between the track and the perpendicular to the sensor, in the plane perpendicular to the sensor and containing the perpendicular to the strip. The optimal projected angle varies between 7° for a pitch of 40 μm and 18° for the largest strip pitch of around 100 μm. The hit resolution is determined from the residual defined as the distance between the hit measurement and the point the fitted track intercepts the sensor which provided the measurement.

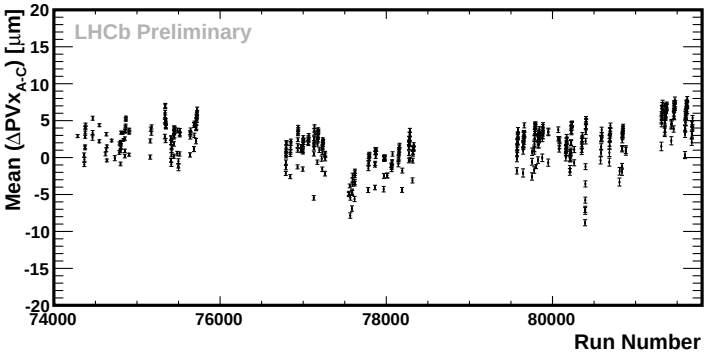

Figure 4: Stability of the VELO half misalignment during 2010.

The resolution has been determined as a function of the strip pitch and the projected track angle as shown in figure 5. The best hit precision is 4 μm for a minimum pitch of 40 μm and an optimal projected angle of 8°.

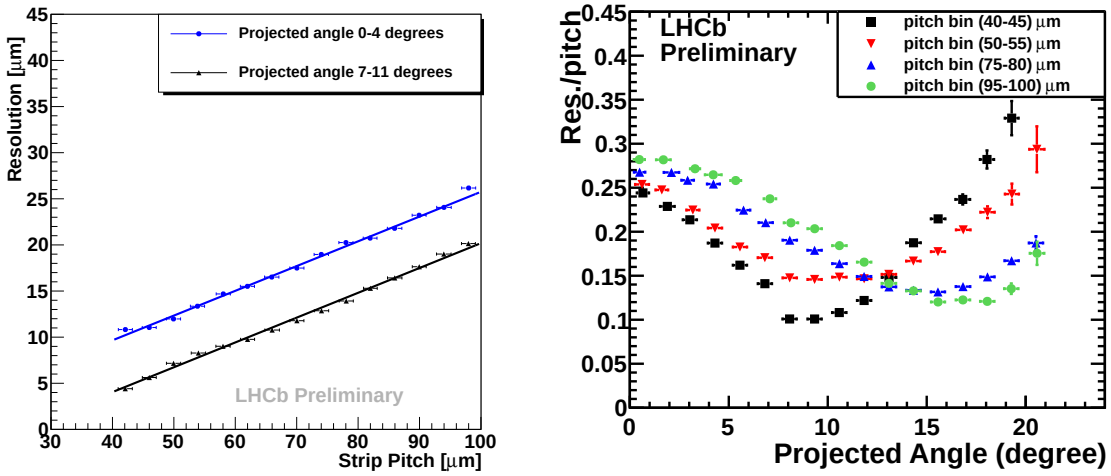

Figure 5: Resolution as a function of strip pitch for different bins of projected angle (left) and residual divided by pitch as a function of the projected angle for different bins of strip pitch (right) measured using 2010 data.

5. Silicon Tracker Performance

The analogue data are transferred to service boxes located in a low radiation area outside the detector acceptance. The data is digitised and then transmitted using VCSEL[1] diodes to the TELL1 boards. The data is pre-processed using FPGAs on the TELL1 board where it undergoes pedestal subtraction, removal of cross-talk, common mode suppression and zero suppression.

The fraction of working channels at the time of the conference was 99.72% and 98.81% for the TT and IT respectively. The main source of inefficiency is caused by the failure of VCSEL diodes

[1] Vertical Cavity Surface Emitting Laser

used in the optical readout[2]. The broken VCSELs can easily be replaced during short shutdowns in the TT as the TT service boxes are easily accessible during short technical stops. Repairs to the IT electronics are much harder due to its location under the IT which requires the detector to be open for access. The IT also has two modules which cannot be configured. Repairs will be made during the long shutdown in 2013.

The signal to noise ratio (S/N) was determined using clusters from tracks reconstructed with momentum greater than 5 GeV. The S/N for the TT was found to be in the range 12 to 15 and is shown in figure 6 for the different strip capacitances. The long and short ladders in IT have a S/N of 16.5 and 17.5 respectively. The distribution of the S/N for all ladders in the IT is shown in figure 6. There is a peak with S/N around 23 for the short ladders in IT as some 410 μm sensors were used instead of the 320 μm sensors during the early module production. The values obtained are within 10-20% of those expected from prototype measurements [7].

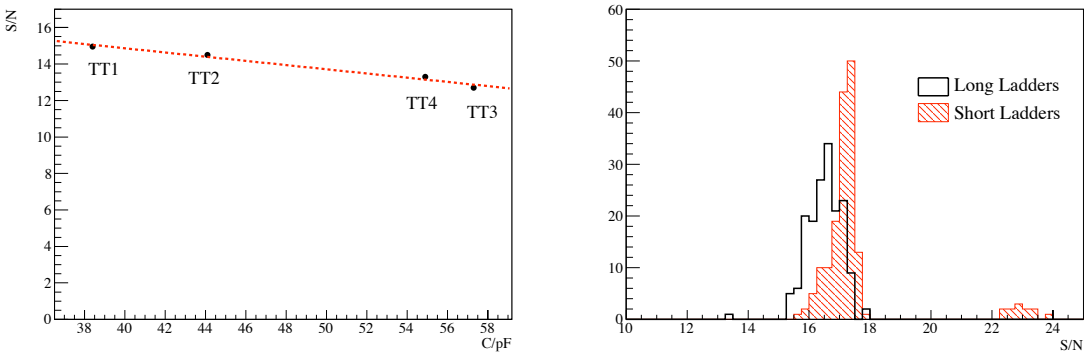

Figure 6: Measured signal to noise ratio as a function of strip capacitance in TT (left) and for different strip lengths in IT (right).

A spatial alignment of the detector was made using a global χ^2 minimisation based on Kalman track residuals [9]. Additional requirements were introduced by using a of sample of decay vertices reconstructed from two or more tracks (or particles) and applying constraints to their invariant mass [11]. The alignment was performed using a sample of invariant mass constrained vertices from $D^0 \to K^-\pi^+$ decays. The unbiased residuals for all clusters on tracks are shown in figure 7 (a) and (b). The unbiased residual is calculated by removing the hit from the track fit and calculating the distance between the hit and the extrapolated track position. The biased residual for a given sensor is defined as the mean of the unbiased residual distribution for this sensor. The distribution of the biased residuals from all sensors is shown in figures 7 (c) and (d). The precision of the alignment procedure is given by the RMS of these distributions and is found to be around 14 μm for both TT and IT. The single hit resolution was extracted by removing the contribution due to the biased sector residuals from the unbiased residuals. The hit resolution was measured to be 59 μm and 50 μm for the TT and the IT respectively.

6. Track Finding Efficiency

The tracking efficiency has been measured with a *tag-and-probe* method using J/Ψ decays [12].

[2]Produced by ULM photonics GmbH (type ULM850-05-TN-USMBOP) [6]

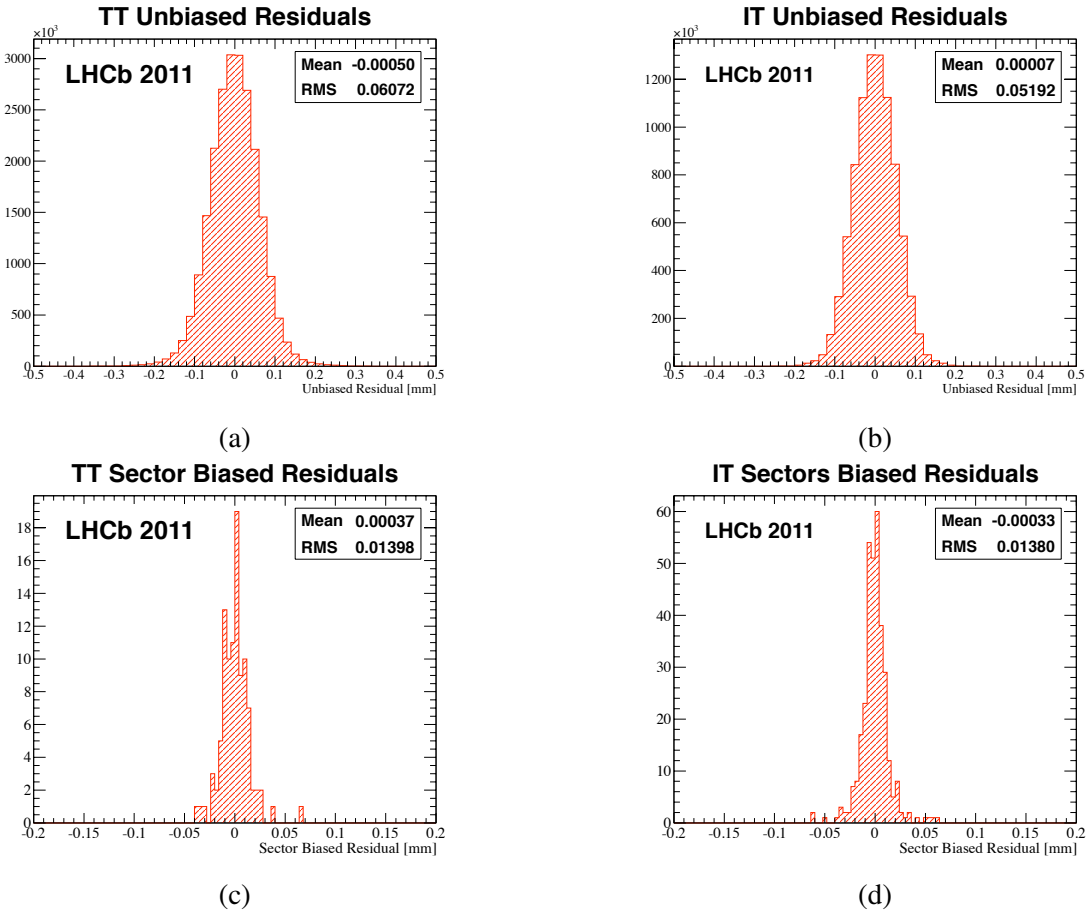

Figure 7: Unbiased cluster residuals for TT (a) and IT (b). Biased sector residuals for TT (c) and IT (d). The calculation of the residuals is described in the text.

The *tag* track is a fully reconstructed muon with hits in all of the tracking stations while the *probe* track is only partially reconstructed using a subset of the tracking sub-detectors. The reconstructed probe particle is required to have enough momentum information such that the invariant mass of the J/Ψ can be determined with high resolution. The probe track is then matched to a fully reconstructed track and the efficiency is defined as the ratio of the number of matched tracks to the the total number of probe tracks. The probe tracks are reconstructed using different combinations of tracking detectors which allow the track finding efficiency to be determined for different track types. The overall efficiency is around 98% and was found to depend on pseudorapidity, η, momentum, p, and event multiplicity. The ratio of the efficiency determined on data to that from the simulation is (100.9$\pm$0.6)% for the data taken in 2011.

7. Physics Performance

The measurement of decay lifetimes of the *b*- and *c*- hadrons requires an accurate reconstruction of the primary vertex (PV) and the decay vertices. The primary vertex resolution depends strongly on the number of tracks used to reconstruct the vertex. The resolution is measured by randomly splitting the track sample in two and reconstructing two independent PVs. The resolu-

tion determined for each track multiplicity is the σ from a Gaussian fit to the distribution of the distance between the two PVs divided by $\sqrt{2}$. The resolution is shown in figure 8 as a function of the number of tracks used in the PV reconstruction. The resolution achieved using 25 tracks to reconstruct an event containing a single PV is (13.1, 12.5, 69.2) μm for the (x, y, z) components. This is close to the design values. For events containing more than one PV, the resolution is slightly worse and is measured to be (14.1, 13.7, 78.3) μm in (x, y, z).

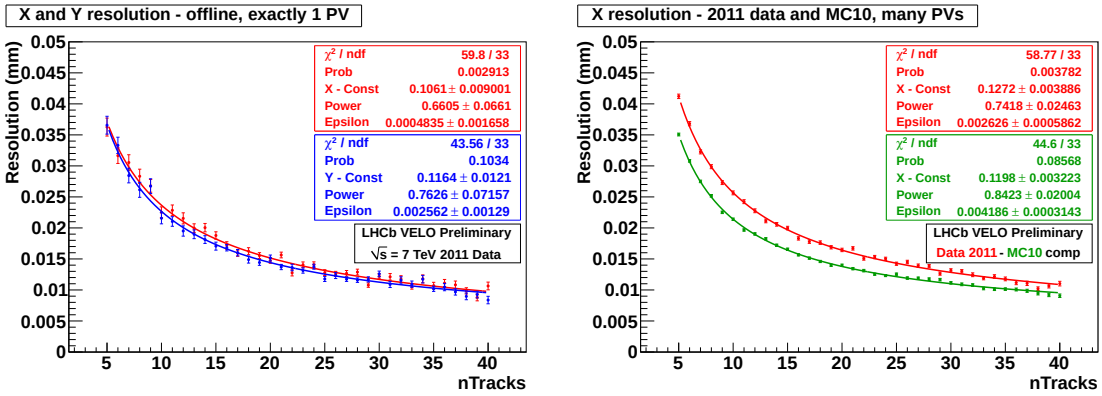

Figure 8: (Left) Primary vertex resolution in x (red) and y (blue) as a function of track multiplicity for events containing a single primary vertex. (Right) Resolution in x as a function of track multiplicity determined on events which contained many PVs for data (red) and simulation (MC10, green).

Another useful variable in the selection of heavy flavour decays is the Impact Parameter (IP). It is defined as the distance of closest approach of a track to the Primary Vertex. Tracks coming from heavy flavour decays typically have larger IPs than those coming from the PV. The IP resolution is governed by three main factors: multiple scattering of particles in detector material; the single hit resolution; and the distance between the PV and first measurement in the detector. The IP resolution can be determined by examining the widths the of IP_X and IP_Y distributions for all tracks where IP_X and IP_Y are the 1-D projections of the IP in x and y respectively. The resolution of IP_X is shown in figure 9 as a function of p_T and $1/p_T$. The resolution is measured to be $\sigma = (13.2 + 24.7/pT)\ \mu m$ for 2011 data. There is a discrepancy between the IP resolutions measured in simulation and data which is probably due to differences between the description of RF foil used in the simulation and the material seen by tracks traversing the detector. Work is ongoing to understand this.

8. Conclusions

The LHCb tracking system works extremely well despite operating under very different conditions compared to its design. Data was collected during 2011 and 2012 with multiple pile-up events at far higher instantaneous luminosities than the design, but with no degradation in the detector peformance. The average pile-up and instantaneous luminosity during 2012 are $\langle\mu\rangle \approx 1.7$ and $\langle\mathscr{L}\rangle \approx 4\times10^{32}/\mathrm{cm}^2/\mathrm{s}$.

The signal to noise ratio for clusters on tracks measured in the VELO is greater than 17 for all sensors. For the TT, the value was measured to be in the range 12 to 15 depending on the strip length. The signal to noise ratio in the IT was found to be 16.5 and 17.5 for the long and short strips respectively.

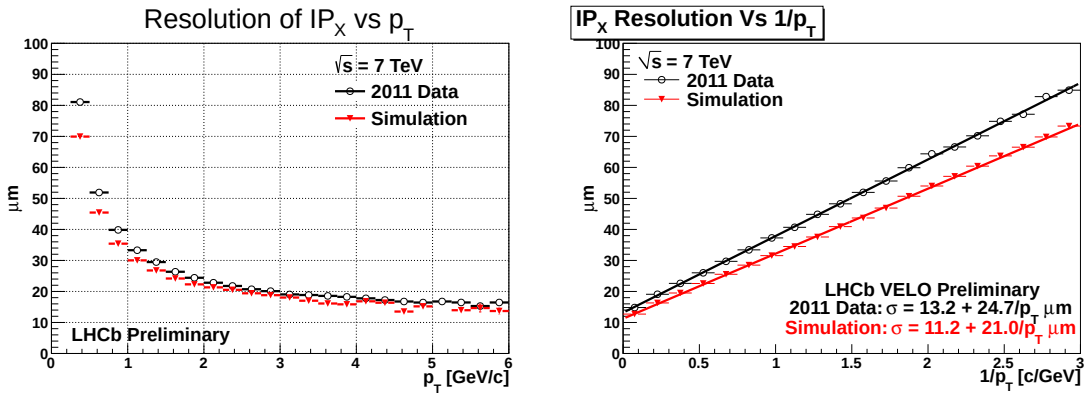

Figure 9: Impact parameter resolution, IP_X as a function of p_T (left) and $1/p_T$ (right).

The best hit precision achieved by the VELO is 4 μm for a minimum pitch of 40 μm and an optimal projected angle of 8°. The measured hit resolution in the TT and IT is 59 μm and 50 μm respectively. The expected resolution in the Silicon Tracker is around 50 μm.

The track finding efficiency has been measured with a tag-and-probe method using $J/\psi \rightarrow \mu^+\mu^-$ decays. The overall efficiency is around 98% for the data collected in 2011 and was found to depend on the momentum and pseudorapidity of the track as well as the event multiplicity. The ratio of the efficiency measured in data to that measured in the simulation is $\varepsilon_{data}/\varepsilon_{MC} = (100.9 \pm 0.6)\%$ for the 2011 data.

The primary vertex resolution was measured and found to be (13.1, 12.5, 69.2) μm in (x, y, z) for events containing a single primary vertex constructed using 25 tracks. This is slightly worse than the resolution expectation from simulation. The resolution is also worse for events with higher pile-up events where it is measured to be (14.1, 13.7, 78.3) μm in (x, y, z).

The impact parameter resolution was measured using the 2011 data and is described by the linear relation $\sigma = (13.2 + 24.7/\mathrm{p_T})$ μm where σ is the resolution and p_T is the transverse momentum. There is still a difference between the value measured in the data and the simulation. Work in ongoing to resolve this discrepancy.

References

[1] The LHCb Detector at the LHC, LHCb Collaboration, JINST 3 S08005 (2008).

[2] LHCb Collaboration, Phys. Lett. B 694, 209-216 (2010).

[3] Particle Data Group, J. Beringer et al., Review of particle physics, Phys. Rev. D86 442 (2012).

[4] N. van Bakel *et al.*, CERN/LHCC 2001-046 (2001)

[5] G. Haefeli *et al.*, Nucl. Inst. Meth., A560, 494 (2006).

[6] http:://http://www.ulm-photonics.de/

[7] M. Agari et al., LHCb-2002-058 (2002).

[8] S. Viret et al., Nucl. Inst. Meth., A596, 157 (2008).

[9] W. Hulsbergen, Nucl. Inst. Meth., A600, 471-477 (2009).

[10] S. Borghi, Nucl. Inst. Meth., A623, 156-158 (2010).

[11] J. Amoraal *et al.*, Application of vertex and mass constraints in track-based alignment, arXiv:1207.4756 [physics.ins-det]

[12] A. Jaeger et al., CERN-LHCb-PUB-2011-025 (2012).